




## Experimental observation of topological quantum criticality

Sonja Barkhofen,<sup>1</sup> Syamsundar De,<sup>1</sup> Jan Sperl<sup>1</sup>,, Christine Silberhorn,<sup>1</sup> Alexander Altland,<sup>2</sup> Dmitry Bagrets,<sup>2</sup> Kun Woo Kim,<sup>3</sup>, and Tobias Micklitz<sup>4</sup>

<sup>1</sup>*Integrated Quantum Optics Group, Institute for Photonic Quantum Systems (PhoQS), Paderborn University, Warburger Straße 100, 33098 Paderborn, Germany*

<sup>2</sup>*Institut für Theoretische Physik, Universität zu Köln, Zùlpicher Straße 77, 50937 Köln, Germany*

<sup>3</sup>*Department of Physics, Chung-Ang University, 06974 Seoul, Republic of Korea*

<sup>4</sup>*Centro Brasileiro de Pesquisas Físicas, Rua Xavier Sigaud 150, Rio de Janeiro 22290-180, Brazil*



(Received 13 January 2023; revised 29 December 2023; accepted 13 May 2024; published 21 August 2024)

We report on a photonic simulator of the critical state forming at the quantum phase transition between topologically distinct Anderson insulator phases. We observe a time-staggered profile in the circular photon polarization, which originates from the interplay of a chiral and sublattice symmetry, and has recently been suggested as a signature for topological Anderson criticality within the setup. We discuss the role of statistical detuning from criticality and show that the controlled breaking of phase coherence removes the signal, revealing its origin in quantum coherence.

DOI: [10.1103/PhysRevResearch.6.033194](https://doi.org/10.1103/PhysRevResearch.6.033194)

### I. INTRODUCTION

Quantum phase transitions between individually gapped topological insulator phases go along with the transient formation of extended critical states. The physical properties of these states are particularly intriguing in cases where static disorder is present, and the gaps of the competing phases are *mobility gaps* rather than the spectral gaps of clean insulators. In this case, topology trumps Anderson localization at the transition point, leading to the emergence of an exotic delocalized state. In this paper we report on a direct experimental observation of signatures of such a state in one dimension, where the effects of Anderson localization are particularly strong.

The presence of disorder in one-dimensional (1D) systems generically causes Anderson localization of single-particle states at microscopically short length scales [1,2]. The single known exception to this rule is quantum criticality between different symmetry-protected topological phases [3,4]. At criticality, the number of topological boundary states changes, and the only way to do so is by hybridization through the bulk [5–7]. This topologically enforced delocalization stabilizes a critical state with exotic properties, including logarithmically slow spreading of wave packages and large sample-to-sample fluctuations of transport observables [8–11].

The observation of such a type of topological quantum criticality is experimentally challenging [12]. It requires precision control over an internal degree of freedom, or “spin,” difficult to achieve, e.g., in ultracold atom setups, otherwise tailored to the observation of Anderson localization [13–15].

Moreover, in the 1D setting the identification of reluctant (logarithmically slow) delocalization appears to require signal observation over exponentially long timescales. We here show that the toolbox of quantum optics experimentation is sufficiently versatile to overcome these challenges. Specifically, we report on the quantum simulation of a 1D *topology driven* localization transition in symmetry class AIII [16,17] within an optical linear network. This network implements discrete time quantum walks of a quantum particle, where the photon polarization defines a spin-1/2 degree of freedom. Effectively one-dimensional hopping is introduced by a time-multiplexing scheme realized through two optical fiber loops of different length (cf. Fig. 1) [18–20]. Finally, tunable polarization plates provide the control required for the definition of topologically nontrivial Anderson insulating phases [19,21,22]. The principal challenge then lies in the observation of a characteristic feature identifying the critical state within the experimentally accessible number of time steps.

In a recent work [23], we defined such a signature, and an experimental protocol for its measurement. The proposal was to monitor a time-staggered profile in the photon polarization as evidence for criticality. We here report on the experimental realization of this protocol. To anticipate the main results, we have observed an alternating signal in the circular photon polarization, demonstrating the presence of a critical state over the maximum number of 14 resolvable time steps. Control measurements with incoherent “dynamic” disorder and numerical control simulations have been performed to exclude measurement errors. However, the walk is too limited in time for a systematic scaling analysis of departures off criticality.

### II. QUANTUM WALK PROTOCOL

We simulate the 1D quantum walk of a spin-1/2 particle, with a single time-step evolution operator

Published by the American Physical Society under the terms of the [Creative Commons Attribution 4.0 International](https://creativecommons.org/licenses/by/4.0/) license. Further distribution of this work must maintain attribution to the author(s) and the published article's title, journal citation, and DOI.

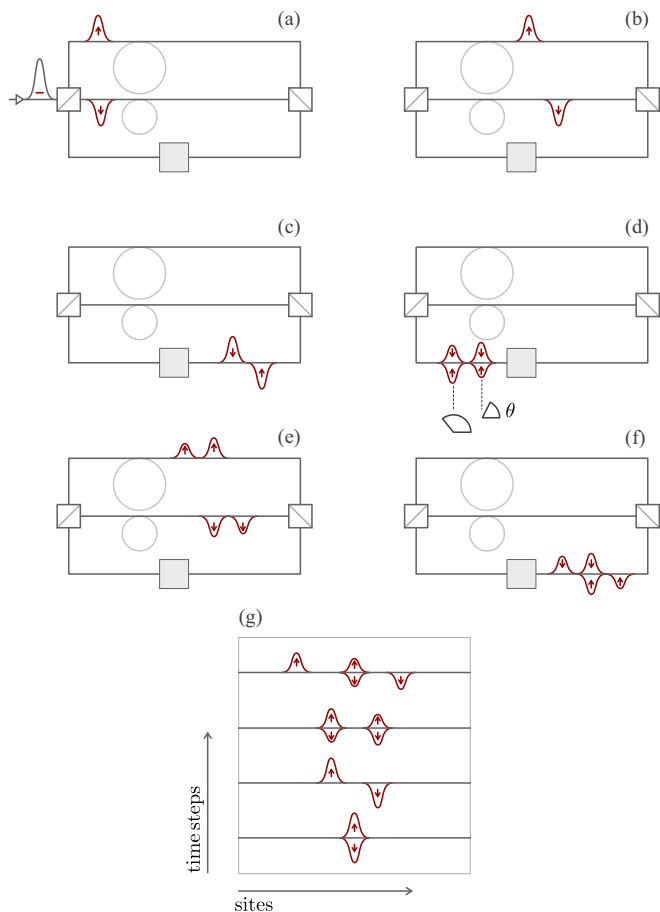


FIG. 1. Optical linear network implementation of the quantum walk (see main text for a discussion). Polarization switches exchanging  $\uparrow$  and  $\downarrow$  states are required for the active in- and outcoupling and here suppressed for simplicity (see the Supplemental Material [24] for details).

$U(\theta) = R(\theta/2)T R(\theta/2)$ . It is composed of the step operator,

$$T = \sum_q (|q+1, \uparrow\rangle\langle\uparrow, q| + |q-1, \downarrow\rangle\langle\downarrow, q|), \quad (1)$$

translating spin-up and spin-down states by one lattice site to the right and left, respectively, and the coin operator,

$$R(\theta) = \sum_q |q\rangle \begin{pmatrix} \cos \theta_q & i \sin \theta_q \\ i \sin \theta_q & \cos \theta_q \end{pmatrix} \langle q|, \quad (2)$$

in the eigenbasis  $|\uparrow, \downarrow\rangle$  of the Pauli matrix  $\sigma_3$ . The operator  $R$  describes spin rotations around the 1-axis, where  $\theta_q$  is an angle randomly drawn at each site from the binary distribution  $\theta_q \in \{\bar{\theta} \pm \theta\}$ .

A schematic of the optical network implementation of  $U(\theta)$  is shown in Fig. 1 (for a more detailed account of the experimental realization, see the Supplemental Material [24]): A state  $|\rightarrow\rangle = \frac{1}{\sqrt{2}}(|\uparrow\rangle - i|\downarrow\rangle)$  with left circular polarization (an eigenstate of  $\sigma_2$ ) is injected into the circuit and split into components of horizontal and vertical polarization ( $\pm 1$  eigenstates of  $\sigma_3$ ,  $|\uparrow\rangle$ , and  $|\downarrow\rangle$ ) by the polarization beam splitter [Fig. 1(a)]. The traversal of fiber loops of different lengths leads to a time delay [Fig. 1(b)], and after recombination

[Fig. 1(c)], a train of two states. An electro-optic modulator (EOM), which acts as a polarization plate with a fast switching rate (hatched box) performs individual polarization rotations  $R(\theta)$ , for the two consecutive pulses of the train, thus completing the first time cycle of the protocol [Fig. 1(d)]. The process is then reinitialized, and after a repeated traversal of loops [Fig. 1(e)] and recombination [Fig. 1(f)], a fourfold superposition is generated. In this way [Fig. 1(g)], repeated traversal of the loop generates a spin-resolved signal and identification of discrete time with a lattice coordinate realizes the quantum walk.

### III. SYMMETRIES

The operator  $U$  possesses the two symmetries,

$$\sigma_2 U \sigma_2 = U^\dagger, \quad S U S = -U, \quad (3)$$

with  $S \equiv \sum_q |q\rangle (-1)^q \langle q|$ . The first of these is a consequence of the definitions Eqs. (1) and (2), and it puts our walk in the chiral symmetry class AIII [25,26]. The second relation states that  $U$  is block off-diagonal in site space. A convenient way to combine the two symmetries is to define the operator  $V = iU$  which likewise is chiral, but with regard to the symmetry operation  $(\sigma_2 S)V(\sigma_2 S) = V^\dagger$ . The consequence of a chiral symmetry is the mirror symmetry of the quasienergy spectrum around the points 0 and  $\pi$  [27]. Since the operators  $U$  and  $V$  are identical up to a shift of their spectrum by  $-\pi/2$  induced by the factor  $i$ , we conclude that the spectrum of our walk is organized around *four* mirror symmetric points  $-\pi/2, 0, \pi/2, \pi$ . In the absence of the coin operation,  $\theta_q = 0$ , we have quasienergy band closings at all four of these energies. It is straightforward to check that finite values  $\theta_q = \bar{\theta}$  “gap out” the points 0 and  $\pi$  (viz., open a gap at the respective quasienergy), and a finite staggering profile  $\theta_s = \theta_q (-1)^q$  those at  $-\pi/2$  and  $\pi/2$ .

### IV. QUANTUM CRITICAL DYNAMICS

Consider a topological phase transition of the operator  $V$ . We recall that in a topological phase defined by a finite value of  $\theta_s$  the system supports states at the critical energies  $\pm\pi/2$ . (We use “critical energy” as shorthand for quasienergy of a critical state with corresponding quasienergy). They are at the same time eigenstates of the chiral symmetry operator,  $\sigma_2 S$ , with eigenvalues  $\pm 1$  and localized at the two opposite boundaries. Upon tuning into a critical configuration, these states leak into the bulk. The same is true in the presence of disorder, where a competition between the topologically enforced state hybridization and Anderson localization leads to an extremely slow type of dynamics known as Sinai diffusion [8,28]. While Sinai diffusion due to its logarithmically slow spreading of the wave packets is beyond observability by currently available means, we here put the emphasis on a different signature of the hybridization process. The eigenstates of our chiral operator  $\sigma_2 S$  have a definite circular polarization profile  $\dots c_{2q-1}|2q-1\rangle|\mp\rangle + c_{2q}|2q\rangle|\pm\rangle + c_{2q+1}|2q+1\rangle|\mp\rangle + \dots$  [29]. In the presence of coin disorder, this rigid correlation between orbital and spin degrees of freedom is not conserved. However, referring to Ref. [23] for microscopic calculations, a finite correlation between circular

polarization and spatial position remains present in the full system of eigenstates of the disordered time-evolution operator at energies close to the critical ones,  $\epsilon = \pm\pi/2$ . Critical states near  $\epsilon = 0, \pi$ , on the other hand, are eigenmodes of  $\sigma_2$ , and show a spatially homogeneous circular polarization profile  $\dots c_{2q-1}|2q-1\rangle|\pm\rangle + c_{2q}|2q\rangle|\pm\rangle + c_{2q+1}|2q+1\rangle|\pm\rangle + \dots$ . On this basis, we expect correlation profiles with either homogeneous or alternating circular polarization supported by states close to the above critical quasienergies. The statistical observation of these correlation profiles defines our approach to the detection of topological quantum criticality.

As a time-resolved observable for their detection, we consider

$$\Delta P(t) \equiv \sum_q [P_{--}(t, q) - P_{+-}(t, q)], \quad (4)$$

where

$$P_{\sigma-}(t, q) = \langle |\langle q, \sigma | U^t | 0, - \rangle|^2 \rangle_{\theta}, \quad \sigma = \pm, \quad (5)$$

is the probability for a photon initialized in  $|0, -\rangle$  to be found after  $t$  time steps at a distance  $q$  in state  $\sigma = \pm$ . The average  $\langle \dots \rangle_{\theta}$  is over randomly drawn binary configurations  $\{\theta_q\}$ . Note that in each time step the walk hops between nearest-neighbor sites. A spatially staggered polarization supported by states at energies  $\pm\pi/2$  will thus show as a temporally staggered contribution  $P(t) = (-1)^t |P(t)|$ , or a peak in its Fourier spectrum at  $\omega = \pi$ . By contrast, the critical states with uniform circular polarization are expected to provide an approximately static excess contribution to  $P(t)$ , and a peak at  $\omega = 0$ .

While the linear optical network provides access to these data, the measurement remains challenging. One reason is that Eq. (4) effectively samples over all quasienergy states, including polarization-uncorrelated states far off the critical energies. We thus anticipate our spectral peaks to sit on a background of data distributed over Fourier space. Second, the small number  $t$  of simulated time steps complicates the fine tuning to the critical point: A random walk of  $t$  time steps typically extends over  $N_t \sim \sqrt{t}$  different sites,  $q \in \text{walk}$ . For small numbers of time steps, averages over the corresponding set of random angles  $\{\theta_q\}_{q \in \text{walk}}$  drawn from the binary distribution  $\{\pm\theta\}$ , are dominated by fluctuations. That is, averages over angles,  $\bar{\vartheta} \equiv \frac{1}{N_t} \sum_{q \in \text{walk}} \theta_q$ , and staggered background,  $\bar{\vartheta}_s \equiv \frac{1}{N_t} \sum_{q \in \text{walk}} (-1)^q \theta_q$ , are both roughly proportional to  $\sim \theta/\sqrt{N_t}$  [30]. We therefore realize an ensemble of states distributed around the critical point  $(\bar{\theta}, \bar{\theta}_s) = (0, 0)$ .

In view of the limited statistics, we did not try to systematically analyze farther departures from criticality and instead benchmark our measurement data against random *noise*, in which the rotation angles are randomly drawn in each step. In this way, we generate effectively time-dependent disorder, for which we expect the dephasing of quantum interference and a reduction to a trivially diffusive walk.

## V. EXPERIMENT AND RESULTS

We obtain the polarization-resolved probability distribution Eq. (5) by recording measurements for 500 realizations of the walk generated by drawing from the binary distribution

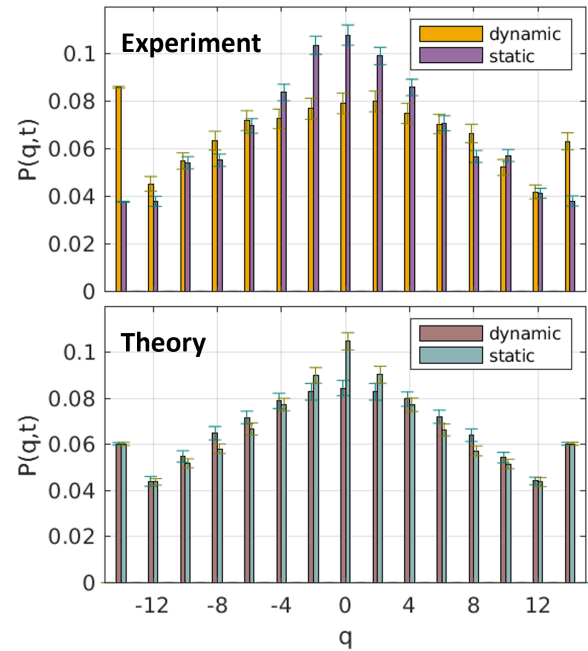


FIG. 2. Total probability distributions  $P(q, t) = P_{--}(t, q) + P_{+-}(t, q)$  of a critical quantum walker with static (violet/green) and dynamic (orange/brown) disorder for  $t = 14$  time steps and upon averaging over 500 different disorder realizations. The experimental distributions (upper panel) are compared to numerical simulations (lower panel) using the same parameters.

$\theta_q \in \{\pm\pi/8\}$ . Figure 2 shows the total probability distribution  $P(t, q) \equiv P_{--}(t, q) + P_{+-}(t, q)$  for the noise and the static randomness protocol, respectively, at  $t = 14$ . The number of time steps that can be simulated is limited due to photon losses, and  $t = 14$  is the limit of the present setup for which we were able to provide reliable data. The quantity  $P(t, q)$  describes the space- and time-dependent probability distribution of the walker, which, at the short time  $t = 14$ , does not show major differences between the two realizations of the protocol. However, closer inspection reveals a different envelope function of the probability distribution, an exponential one indicating the onset of Anderson localization in the static case versus the Gaussian profile of a classical random walk for random noise [19]. (The peaks at  $q = \pm 14$  are due to a small fraction of quasiballistically propagating photons, and disappear for larger numbers of time steps [24].)

The left panel of Fig. 3 shows the spin polarization Eq. (4) extracted via the same protocol for times between  $t = 5$  and 14 and static disorder. The data (purple) shows the expected tendency to staggering in qualitative agreement with numerical simulation (green). (We checked that other choices of time windows lead to similar results.) The middle panel of Fig. 3 shows the resulting power spectrum,  $S(\omega) = |\Delta\bar{P}(\omega)|^2 / \sum_{\omega} |\Delta\bar{P}(\omega)|^2$ , where  $\Delta\bar{P}(\omega) = \sum_{t=5}^{14} e^{i\omega t} \langle \Delta P(t) \rangle_{\theta}$ . For comparison, we show in the right panel of Fig. 3 the corresponding power spectrum for *dynamic* binary disorder. The latter has a structureless random pattern with contributions of the same order from all frequencies, as expected for a noisy circular photon polarization. In contrast, the circular polarization for static disorder shows the

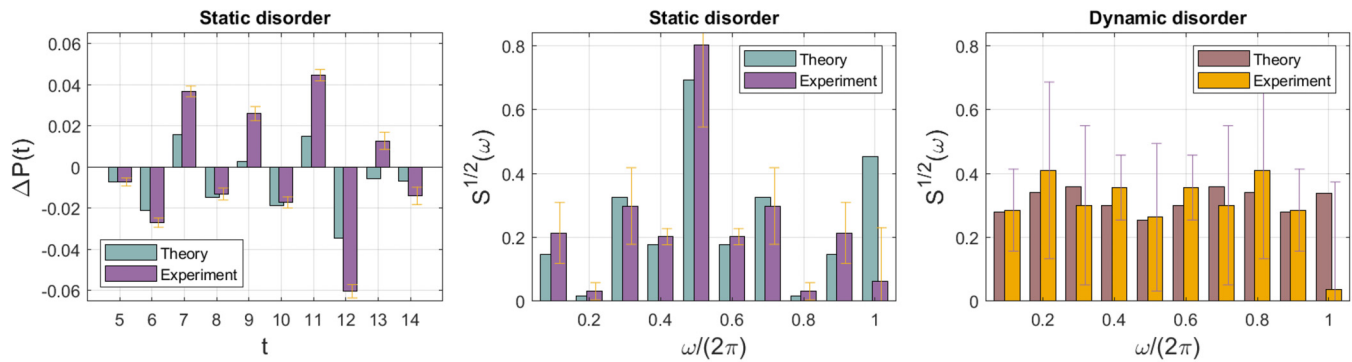


FIG. 3. Circular photon polarization  $\Delta P(t)$  as a function of time steps, Eq. (4), for a quantum walk with static disorder (left panel), and the resulting power spectrum  $\sqrt{S(\omega)}$  (middle panel). In both panels the experimental polarization (purple) is compared to simulation using the same parameters (green). Right panel: Power spectrum for a quantum walk with dynamic disorder from experiment (orange) and simulation (gray). All data are obtained from averaging over 500 realizations of random binary angle configurations.

time-staggering predicted for the topological quantum critical state. The time-staggering is also witnessed by the pronounced peak at  $\omega = \pi$  in the power spectrum. The contribution at  $\omega = 0$  observed in experiment and simulation, on the other hand, is smaller than expected, which reflects the limited statistics, i.e., is a manifestation of fluctuations. To further elaborate this point, we repeated numerical simulations of ensembles of 500 random binary static and dynamic angle configurations for 1000 times. We confirm that the resulting distribution of values  $S(0), S(\pi)$  is centered around large values, either at  $\omega = 0, \omega = \pi$ , or both. The average power spectrum for the entire ensemble of  $1000 \times 500$  binary angle configurations exhibits the expected two-peak structure, with peaks at  $\omega = 0, \pi$  dominating over an otherwise approximately flat background (see Supplemental Material for details [24]).

## VI. DISCUSSION

We have realized a photonic simulator that provides the direct experimental probe of the critical states at a 1D topological Anderson localization phase transition. Our optical linear network simulates the 1D quantum walk of a spin-1/2 particle in a class AIII system. The role of spin is taken by the photon polarization and the architecture allows to fully access and monitor the latter. Upon tuning to the critical point separating two topologically distinct Anderson insulating phases, we observe a time-staggered circular polarization of the photons. The latter is supported by critical states in systems with sublattice symmetry, and has been recently suggested as a signature of quantum critical dynamics. We do not observe a static contribution to the circular photon polarization, also predicted as a signature for topological criticality. We relate its absence to large statistical fluctuations due to a limited number of time steps, and requiring averaging over ensembles orders of magnitude larger than the present. To reveal the peak's origin in quantum coherence we repeated the experiment for

time-dependent noise, or “dephasing disorder.” In this case, the power spectrum has a structureless random pattern with contributions of the same order from all frequencies, as expected for a noisy circular photon polarization.

A crucial step for future experiments is to increase the number of simulated time steps. This should allow for an observation of the two peak structures already in smaller ensembles. Ideally, one would then like to monitor scaling phenomena induced by controlled detuning from criticality and symmetry breaking, for which the currently realizable signal times are still too short for a reasonable statistical analysis. Irrespective of these limitations, we believe that the current experiment shows the possibilities offered by reconfigurable optical linear networks with fast switchability, promising interesting perspectives for the simulation of topological quantum matter in the presence of engineered randomness.

Data-analysis, and codes used in the generation of the figures are available in Zenodo with the identifier 10.5281/zenodo.12799226 [32].

## ACKNOWLEDGMENTS

The Integrated Quantum Optics group acknowledges support by the ERC project QuPoPCoRN (Grant No. 725366). T.M. acknowledges financial support by Brazilian agencies CNPq and FAPERJ. A.A. and D.B. acknowledge partial support from the Deutsche Forschungsgemeinschaft (DFG) within the CRC network TR 183 (Project No. 277101999) as part of projects A01 and A03. K.W.K. acknowledges the support by the National Research Foundation of Korea (NRF) grant funded by the Korea government (MSIT) (Grant No. 2020R1A5A1016518). A.A. and T.M. acknowledge partial support from the Deutsche Forschungsgemeinschaft (DFG) under Germany's Excellence Strategy Cluster of Excellence Matter and Light for Quantum Computing (ML4Q) EXC 2004/1 3905347.

[1] P. W. Anderson, Absence of diffusion in certain random lattices, *Phys. Rev.* **109**, 1492 (1958).

[2] E. Abrahams, P. W. Anderson, D. C. Licciardello, and T. V. Ramakrishnan, Scaling theory of localization: Absence of

- quantum diffusion in two dimensions, *Phys. Rev. Lett.* **42**, 673 (1979).
- [3] D. Khmel'nitskii, Quantization of Hall conductivity, *JETP Lett.* **38**, 552 (1983).
- [4] F. Evers and A. D. Mirlin, Anderson transitions, *Rev. Mod. Phys.* **80**, 1355 (2008).
- [5] A. Altland, D. Bagrets, L. Fritz, A. Kamenev, and H. Schmiiedt, Quantum criticality of quasi-one-dimensional topological Anderson insulators, *Phys. Rev. Lett.* **112**, 206602 (2014).
- [6] I. Mondragon-Shem, T. L. Hughes, J. Song, and E. Prodan, Topological criticality in the chiral-symmetric AIII class at strong disorder, *Phys. Rev. Lett.* **113**, 046802 (2014).
- [7] J. Song and E. Prodan, AIII and BDI topological systems at strong disorder, *Phys. Rev. B* **89**, 224203 (2014).
- [8] L. Balents and M. P. A. Fisher, Delocalization transition via supersymmetry in one dimension, *Phys. Rev. B* **56**, 12970 (1997).
- [9] A. Altland, D. Bagrets, and A. Kamenev, Topology versus Anderson localization: Nonperturbative solutions in one dimension, *Phys. Rev. B* **91**, 085429 (2015).
- [10] A. K. H. Zhang, The anatomy of topological Anderson transitions, *Phys. Rev. B* **108**, 224201 (2023).
- [11] For typical samples, e.g., thermal and electric conductivities vanish, while averages over large ensembles are dominated by rare good conductors, bringing about finite *average* conductivities at topological criticality.
- [12] For a recent observation of a topological Anderson insulator phase in a 1D lattice of ultracold atoms, see, e.g., Ref. [31].
- [13] J. Chabé, G. Lemarié, B. Grémaud, D. Delande, P. Szriftgiser, and J. C. Garreau, Experimental observation of the Anderson metal-insulator transition with atomic matter waves, *Phys. Rev. Lett.* **101**, 255702 (2008).
- [14] C. Hainaut, I. Manai, J.-F. Clément, J. C. Garreau, P. Szriftgiser, G. Lemarié, N. Cherroret, D. Delande, and R. Chicireanu, Controlling symmetry and localization with an artificial gauge field in a disordered quantum system, *Nat. Commun.* **9**, 1382 (2018).
- [15] J. Billy, V. Josse, Z. Zuo, A. Bernard, B. Hambrecht, P. Lugan, D. Clément, L. Sanchez-Palencia, P. Bouyer, and A. Aspect, Direct observation of Anderson localization of matter waves in a controlled disorder, *Nature (London)* **453**, 891 (2008).
- [16] A. Altland and M. R. Zirnbauer, Nonstandard symmetry classes in mesoscopic normal-superconducting hybrid structures, *Phys. Rev. B* **55**, 1142 (1997).
- [17] P. Heinzner, A. Huckleberry, and M. R. Zirnbauer, Symmetry classes of disordered fermions, *Commun. Math. Phys.* **257**, 725 (2005).
- [18] A. Schreiber, K. N. Cassemiro, V. Potoček, A. Gábris, P. J. Mosley, E. Andersson, I. Jex, and C. Silberhorn, Photons walking the line: A quantum walk with adjustable coin operations, *Phys. Rev. Lett.* **104**, 050502 (2010).
- [19] A. Schreiber, K. N. Cassemiro, V. Potoček, A. Gábris, I. Jex, and C. Silberhorn, Decoherence and disorder in quantum walks: From ballistic spread to localization, *Phys. Rev. Lett.* **106**, 180403 (2011).
- [20] T. Nitsche, S. Barkhofen, R. Kruse, L. Sansoni, M. Štefaňák, A. Gábris, V. Potoček, T. Kiss, I. Jex, and C. Silberhorn, Probing measurement-induced effects in quantum walks via recurrence, *Sci. Adv.* **4**, eaar6444 (2018).
- [21] S. Barkhofen, T. Nitsche, F. Elster, L. Lorz, A. Gábris, I. Jex, and C. Silberhorn, Measuring topological invariants in disordered discrete-time quantum walks, *Phys. Rev. A* **96**, 033846 (2017).
- [22] S. Barkhofen, L. Lorz, T. Nitsche, C. Silberhorn, and H. Schomerus, Supersymmetric polarization anomaly in photonic discrete-time quantum walks, *Phys. Rev. Lett.* **121**, 260501 (2018).
- [23] D. Bagrets, K. W. Kim, S. Barkhofen, S. De, J. Sperling, C. Silberhorn, A. Altland, and T. Micklitz, Probing the topological Anderson transition with quantum walks, *Phys. Rev. Res.* **3**, 023183 (2021).
- [24] See Supplemental Material at <http://link.aps.org/supplemental/10.1103/PhysRevResearch.6.033194> for a more detailed description of the experimental implementation, a discussion of the long time probability distributions, and a comment on the statistical detuning.
- [25] J. K. Asbóth, Symmetries, topological phases, and bound states in the one-dimensional quantum walk, *Phys. Rev. B* **86**, 195414 (2012).
- [26] J. K. Asbóth and H. Obuse, Bulk-boundary correspondence for chiral symmetric quantum walks, *Phys. Rev. B* **88**, 121406(R) (2013).
- [27] When  $U|\psi_n\rangle = e^{-i\epsilon_n}|\psi_n\rangle$ , using the chiral symmetry relation in Eq. (3),  $U\sigma_2|\psi_n\rangle = e^{i\epsilon_n}\sigma_2|\psi_n\rangle$ . This implies that the quasienergy spectrum is mirror symmetric around  $\epsilon = 0, \pi$ . Likewise, the relation  $(\sigma_2 S)V(\sigma_2 S) = V^\dagger$  implies that the quasienergy spectrum of  $U = Ve^{-i\pi/2}$  is mirror symmetric around  $\epsilon = -\pi/2, \pi/2$ .
- [28] D. Bagrets, A. Altland, and A. Kamenev, Sinai diffusion at quasi-1D topological phase transitions, *Phys. Rev. Lett.* **117**, 196801 (2016).
- [29] Here,  $|\pm\rangle = \frac{1}{\sqrt{2}}(|\uparrow\rangle \pm i|\downarrow\rangle)$  are the eigenstates of  $\sigma_2$ .
- [30]  $N_l = \sum_{q \in \text{walk}}$  here is the normalization.
- [31] E. J. Meier, F. A. An, A. Dauphin, M. Maffei, P. Massignan, T. L. Hughes, and B. Gadway, Observation of the topological Anderson insulator in disordered atomic wires, *Science* **362**, 929 (2018).
- [32] S. Barkhofen, S. De, J. Sperling, C. Silberhorn, A. Altland, D. Bagrets, K. W. Kim, and T. Micklitz, Data and code for “Experimental observation of topological quantum criticality” (matfiles, matlab script, and figures) [Data set] (2024), Zenodo, doi:10.5281/zenodo.12799226.